

Data driven initial model estimation with application to marine CSEM data

Rune Mittet and Lodve Berre, EMGS

SUMMARY

Initial model estimation can be fully data driven. Normally only one inversion run is required to achieve a good estimate for a smooth initial model with this approach. The scheme saves the operator in charge of the processing from repeated tests to find a proper initial model. It is very common in a production setting that several initial models are tested by the operator for each survey dataset. Thus there is a search not only for the final model but also for the initial model. These initial-model tests have a fairly high cost since they are full-scale inversions. A data driven start model generation approach has the potential to improve marine CSEM imaging, especially in the deeper sections. A real data test from Brazil confirms the potential, the approach is giving a more focused inversion that has a better match with a priori information regarding reservoir placement, both laterally and in depth.

INTRODUCTION

Marine controlled-source electromagnetic data (MCSEM) data are as a rule “imaged” by full waveform inversion (FWI). The end result of the inversion is a resistivity cube. Seismic imaging techniques like depth migration and reverse time migration are not effective since MCSEM data are dominated by refractions and wave-guide contributions (Mittet, 2015). Sometimes FWI is portrayed as a fully automatic procedure. It is not so in a production setting. The large scale 3D nature of this inverse problem precludes global optimization schemes and some sort of local optimization scheme is forced. The local optimization schemes can roughly be divided into gradient based schemes and Gauss-Newton (GN) schemes where also a Hessian approximation is used predict the update. Both types of scheme are usually designed to accept only updates that reduce the error functional. In this way local schemes become dependent on the initial model. For MCSEM our experience is that GN schemes are more robust than gradient based schemes with respect to the choice of initial model, but GN schemes are far from independent of the initial model. A consequence is that it is very common in a production setting that several initial models are tested by the operator for each survey dataset. Thus there is a search not only for the final model but also for the initial model. Unless proper tools are available it may be that the search for the initial model requires more human and computer resources than the search for the final model.

These initial-model tests have a fairly high cost since they are full scale inversions. They tend to use cluster resources on a large scale. Our general experience is that a half space as initial model is too far from the true model to give optimal final models. On the other hand, it may be dangerous to put too much structure into the start model. If that structure information is false, then the inverse scheme may struggle to remove

it to a sufficient degree. A smooth start model is advantageous for MCSEM inversion as is often the case also for seismic inversion. For production work we see that a start model with a gradient in resistivity from the seabed and down performs much better than a half-space model, but it may be possible to perform even better if the search for the initial model is more directly data driven.

The scheme discussed below is a data-driven parametric inversion for a smooth initial model. The parametrized function space ensures the smoothness. The scheme uses a subset of all available receivers in a survey. Typical inline and crossline receiver separations are 5 km, however all towlines are used.

THEORY

Our objective is to construct a smooth resistivity model with a limited number of optimization parameters. The seawater part of the model, including bathymetry variations is kept fixed during all iterations. The parametrized model will have 3D variations. The lateral variations will be described by bivariate polynomials up to second order in the two horizontal coordinates x and y . These polynomials will be multiplied by functions that either cover the total model volume or by spatially bandlimited depth dependent functions. The key function used to describe the smooth depth dependence is the Fermi distribution, \mathcal{F} . The Fermi distribution can be expressed as,

$$\mathcal{F}(z, z_{\mu}^{(1)}, z_w^{(1)}) = \left(1 + e^{\frac{(z - z_{\mu}^{(1)})}{\beta z_w^{(1)}}} \right)^{-1}, \quad (1)$$

where z is the depth coordinate. The parameter $z_{\mu}^{(1)}$ is usually called the Fermi energy or the chemical potential, here it will be called the transition depth. The general behavior of the Fermi distribution is that $\mathcal{F} = 1$ for $z < z_{\mu}^{(1)}$ and $\mathcal{F} = 0$ for $z > z_{\mu}^{(1)}$. A value of $\beta = 0.144$ lets $z_w^{(1)}$ roughly represent the width of the transition zone. The Fermi distribution is used at the top of the formation and immediately below the seabed. Layers in the middle of the formation are represented by the bandlimited boxcar distribution. This function can be expressed as the sum of two Fermi distributions,

$$\mathcal{B}(z, z_{\mu}^{(i)}, z_w^{(i)}, z_{\mu}^{(i+1)}, z_w^{(i+1)}) = \mathcal{F}(z, z_{\mu}^{(i+1)}, z_w^{(i+1)}) - \mathcal{F}(z, z_{\mu}^{(i)}, z_w^{(i)}), \quad (2)$$

where $z_{\mu}^{(i)}$ and $z_w^{(i)}$ are the transition depth and transition width at the top of the layer and $z_{\mu}^{(i+1)}$ and $z_w^{(i+1)}$ are the transition depth and transition width at the bottom of the layer. A bandlimited Heaviside step function is used to terminate the layer structure. The bottom layer is denoted N_L , but the Heaviside step function is forced to have the same transition depth and width as the bottom part of the boxcar distribution in the layer above,

$$\mathcal{H}(z, z_{\mu}^{(N_L-1)}, z_w^{(N_L-1)}) = 1 - \mathcal{F}(z, z_{\mu}^{(N_L-1)}, z_w^{(N_L-1)}). \quad (3)$$

Data driven initial model

Examples of the layer functions are shown in Figure 1.

We can let the transition depths, $z_{\mu}^{(k)}$, be independent of lateral position if the seabed is flat, however, MCSEM surveys are often conducted in areas with large bathymetry variations. In that case it is not unreasonable to assume that there is a trend in the earth layering that follows the bathymetry variations, at least for the shallower part of the subsurface. Our choice is

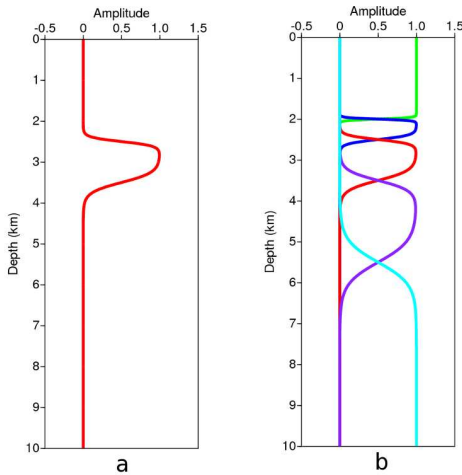


Figure 1: Depth profile of layer function when all amplitude factors equals unity. a) Boxcar function for the third layer. b) Fermi function (green) for the top layer. Heaviside function (cyan) for the bottom layer. The intermediate layers are parametrized with Boxcar function. The layer function is everywhere unity when the amplitudes are unity.

to let the transition depth depend on the lateral position. We define the smoothed bathymetry profile as $z_B(x, y)$. This profile is obtained by lowpass filtering the true bathymetry profile. Transition depths can then be defined as,

$$z_{\mu}^{(k)} \rightarrow z_{\mu}^{(k)}(x, y) = z_B(x, y) + z_{\Delta}^{(k)}, \quad (4)$$

where the $z_{\Delta}^{(k)}$ is independent of lateral position. The layering of the model is then forced to follow the smoothed bathymetry profile. This may be reasonable for the large scale structure of the shallow subsurface but may be less justified with increasing depth. However, we let each layer function be proportional to a bivariate polynomial, a bilinear example is,

$$\begin{aligned} \mathcal{L}^{(k)}(x, y) &= a_1^{(k)} + a_2^{(k)}(x - x_C) + a_3^{(k)}(y - y_C) \\ &+ a_4^{(k)}(x - x_C)(y - y_C) \end{aligned} \quad (5)$$

where (x_C, y_C) is the lateral midpoint of the 3D resistivity model. The degree of the polynomial is a user choice and can be zeroth, first or second order. The polynomial coefficients are the

optimization parameters for the inversion problem. Obviously, a zeroth order polynomial gives few parameters to estimate. The layer thicknesses and transition widths increase logarithmically with depth but are only adjustable prior to the start up of the inversion.

We next expand the layer function \mathcal{L} with two more elements, such that,

$$\begin{aligned} \mathcal{L}^{(1)}(x, y, z, z_{\mu}^{(1)}(x, y), z_w^{(1)}) &= \mathcal{F}(z, z_{\mu}^{(1)}(x, y), z_w^{(1)}), \\ \mathcal{L}^{(2)}(x, y, z, z_{\mu}^{(2)}(x, y), z_w^{(2)}) &= \mathcal{B}(z, z_{\mu}^{(1)}(x, y), z_w^{(1)}, z_{\mu}^{(2)}(x, y), z_w^{(2)}), \\ \mathcal{L}^{(3)}(x, y, z, z_{\mu}^{(3)}(x, y), z_w^{(3)}) &= \mathcal{B}(z, z_{\mu}^{(2)}(x, y), z_w^{(2)}, z_{\mu}^{(3)}(x, y), z_w^{(3)}), \\ &\dots\dots\dots = \dots\dots\dots, \\ \mathcal{L}^{(N_L)}(x, y, z, z_{\mu}^{(N_L)}(x, y), z_w^{(N_L)}) &= \mathcal{H}(z, z_{\mu}^{(N_L-1)}(x, y), z_w^{(N_L-1)}), \end{aligned} \quad (6)$$

and

$$\begin{aligned} \mathcal{L}^{(N_L+1)}(x, y, z, z_{\mu}^{(N_L+1)}(x, y), z_w^{(N_L+1)}) &= 1.0, \\ \mathcal{L}^{(N_L+2)}(x, y, z, z_{\mu}^{(N_L+2)}(x, y), z_w^{(N_L+2)}) &= z - z_B(x, y). \end{aligned} \quad (7)$$

The two last terms allow a for a gradient behavior of the resistivity model independent of the layer structure. The vertical resistivity model can now be expressed,

$$\rho_v(x, y, z, Z_{\mu}, Z_w) = \sum_{k=1}^{N_L+2} \mathcal{L}^{(k)}(x, y) \mathcal{L}^{(k)}(x, y, z, z_{\mu}^{(k)}(x, y), z_w^{(k)}). \quad (8)$$

The parametrization of the horizontal resistivity model has the same form as the parametrization of the vertical resistivity model but the parameters may differ. The optimization scheme has good sensitivity to the parametrization. Formally we can now collect all the amplitude factors $a_i^{(k)}$ for the vertical and $\tilde{a}_i^{(k)}$ for the horizontal resistivity model in a parameter vector p . The 3D resistivity models are a function of this parameter vector only.

Let \mathbf{x}_r be the receiver position, \mathbf{x}_s the source position, ω the angular frequency and i a horizontal component for the field $F_i(\mathbf{x}_r, \mathbf{x}_s, \omega)$, where F_i can be electric field E_i or magnetic field H_i . We denote the observed fields $F_i^{Obs}(\mathbf{x}_r, \mathbf{x}_s, \omega)$. The predicted field depends on the parameter vector p so for the predicted fields at iteration n we write $F_i^{Prd}(\mathbf{x}_r, \mathbf{x}_s, \omega | p)$. The uncertainty in the observed data is $\delta F_i(\mathbf{x}_r, \mathbf{x}_s, \omega)$. The sum over $[\mathbf{x}_r, \mathbf{x}_s, \omega, i, F]$ is then the sum over all observations. A smooth model that fits the observed data can be estimated by minimizing the error functional $\varepsilon(p)$,

$$\begin{aligned} \varepsilon(p) &= \sum_{\mathbf{x}_r, \mathbf{x}_s, \omega, i, F} \eta^2(\mathbf{x}_r, \mathbf{x}_s, \omega, i, F), \\ \eta(\mathbf{x}_r, \mathbf{x}_s, \omega, i, F) &= \frac{\sqrt{\Delta F_i^*(\mathbf{x}_r, \mathbf{x}_s, \omega | p) \Delta F_i(\mathbf{x}_r, \mathbf{x}_s, \omega | p)}}{\delta F_i(\mathbf{x}_r, \mathbf{x}_s, \omega)}, \\ \Delta F_i(\mathbf{x}_r, \mathbf{x}_s, \omega | p) &= F_i^{Obs}(\mathbf{x}_r, \mathbf{x}_s, \omega) - F_i^{Prd}(\mathbf{x}_r, \mathbf{x}_s, \omega | p). \end{aligned} \quad (9)$$

The above optimization problem is solved with the Levenberg-Marquardt algorithm. The Jacobian elements are estimated by

Data driven initial model

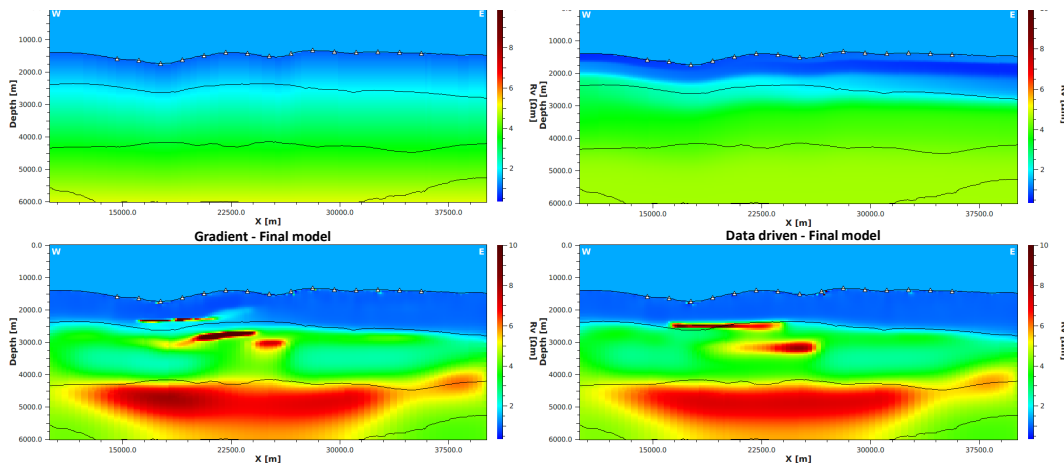


Figure 2: Initial and final models. Left is for gradient start model and right is for data driven start model estimation. Initial model at the top, final models at the bottom.

a finite-difference technique. For the examples to follow, $N_L = 5$ and bilinear polynomials were used such that 56 parameters must be estimated for a vertical plus a horizontal resistivity model.

RESULTS

In order to test the procedure, we forward modeled synthetic data in a layered model containing three different targets at various burial depths and with different thicknesses and resistivities. Two of the targets were stacked on top of each other, with 800 meter separation. Prior to inversion, realistic synthetic noise were added to the data.

The data set was first inverted with our 3D Gauss-Newton scheme, using a gradient start model close to the true model and next using a smooth start model estimated from the data itself. Both inversions were set up with the same parameters, and converged to a misfit level equal to the uncertainty level in the data given by the added noise. Both inversions recreated the background resistivity very well. However, the inversion using the estimated start model was able to separate and image the stacked targets, whereas the inversion using the gradient model struggled in this part of the model and introduced artifacts. Depth placement of the targets is also closer to the true model using the start model based on parametric inversion. Initial and final models are given in Figure 2.

The approach has been tested on a real multi-client data set acquired in 2012 offshore Brazil in the Sergipe-Alagoas Basin, as indicated in Figure 3. The survey consists of 232 receivers in a staggered 2x2 km grid and 15 towlines with 2 km spacing, covering an area of 800 km². This area includes the major Muriu and Moita Bonita discoveries - there is thus ample well control in the area, making it well suited for testing the approach in an actual exploration setting. Both Muriu and Moita Bonita are turbidite sandstone discoveries, situated in the Early Cretaceous section approximately 2500-3000 m below the mudline.

The cross-sections in Figure 4, marked with the red line in Figure 3, covers two wells (3-BRSA-1244-SES to the north and 3-BRSA-1296-SES to the south) which encountered light oil and reservoirs with good permeability and porosity conditions.

Two initial models were tested in this exercise. One where we used a gradient model derived from 2.5D Gauss-Newton inversions. Several towlines were used and the results were interpolated. Only inline data contributed with this procedure. The second initial model was the result of the parametrized inversion scheme described in the previous section. The input to the data driven start model estimation was a decimated version of the complete data set, using 32 receivers spaced 6 km apart, but including all 15 towlines, such that azimuth data contributed to the optimization. Two Gauss-Newton inversion runs were then performed, including all the receivers and all the towlines. Inversion and regularization parameters were identical - the only difference between the two runs was the start model.

As can be seen in Figure 4, the two start models are not radically different, though the data driven model includes a shallow, low resistive layer not captured by the gradient model as well as being more resistive in the deeper parts around and below the discovery interval. The deepest horizon shown in these figures is mapped from legacy 2D seismic data acquired by Veritas and represents a feature near the Base Campanian, while the upper horizon is the same surface shifted up 800 m in order to represent the prospective interval. It is important to note that these horizons have not been used in the inversion process, and only serve as a visual guide when interpreting the results. The initial RMS data misfit from the gradient model was 6.04 compared to 4.63 for the data driven model.

Both inversion runs converged towards the same RMS data misfit of 1.0, and using a similar amount of iterations. In the shallow section above the prospective level, both inversions seem to recover similar resistive features. However, when inspecting the prospective level in light of what we know from the seismic data and the wells in the area, we observe that the final model from the data driven approach is more focused

Data driven initial model

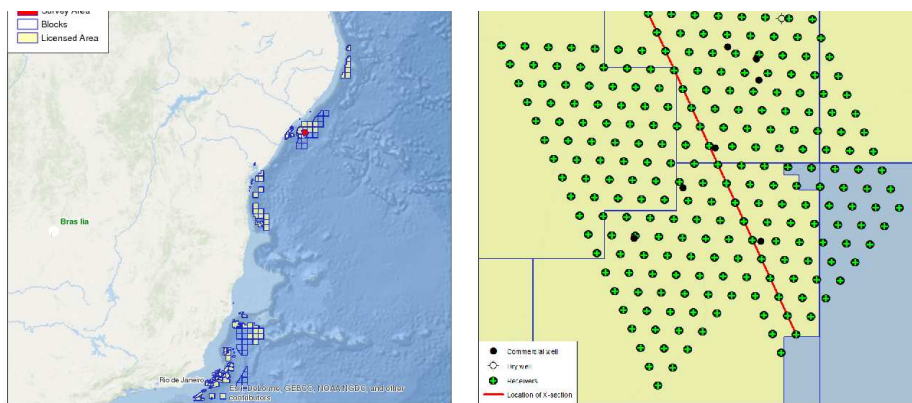


Figure 3: Survey overview to the left and survey layout to the right.

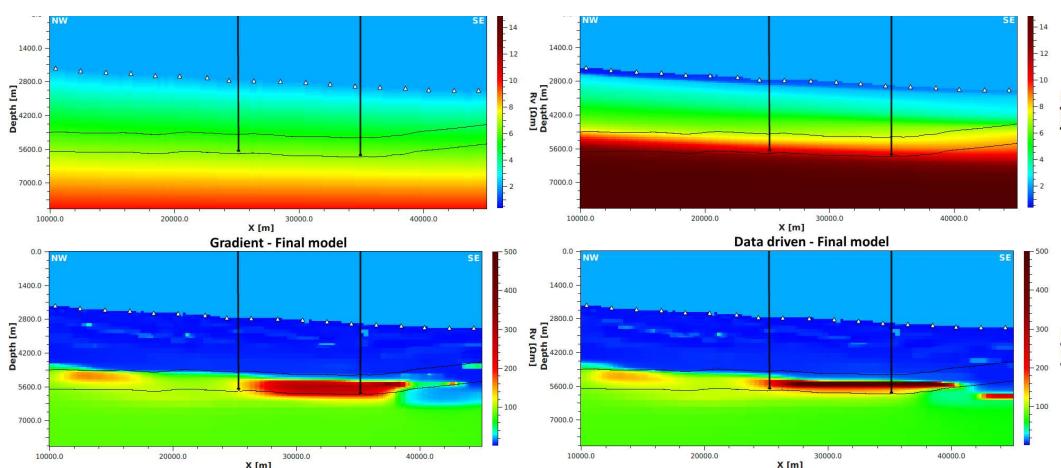


Figure 4: Initial and final models. Left is for gradient start model and right is for data driven start model estimation. Initial model at the top. Final models at the bottom.

and has been able to place the resistive anomalies more appropriately in depth. We also see that the lateral distribution differs slightly, especially at the northern 3-BRSA-1244-SES well, where the final model starting from the data driven initial model estimate has a more distinct anomaly than the final model starting from the gradient model.

We also observe discrepancies in the south eastern part of the cross-section, where the gradient approach has recovered a weak, shallow resistor (2000 m BML) above a deeper conductive section, while the data driven approach has recovered a considerably stronger resistive anomaly and placed it deeper, within the conductive section. However, due to the lack of data points at the edge of the survey, this discrepancy is well within the expected uncertainty at the edge of the survey and would need further testing before doing interpretation at that location.

deeper sections. A real data test from Brazil confirms the potential, the approach, giving a more focused inversion that has a better match with a priori information regarding reservoir placement, both laterally and in depth.

CONCLUSIONS

We see that a data driven start model generation approach has the potential to improve MCSEM imaging, especially in the

REFERENCES

Mittet, R., 2015, Seismic wave propagation concepts applied to the interpretation of marine controlled-source electromagnetic: *Geophysics*, **80**, no. 2, E63–E81, <https://doi.org/10.1190/geo2014-0215.1>.